Macromolecular Symposia
www.ms-journal.de

# Preparation and Characterization of Polymeric Microfibers of PLGA and PLGA/PPy Composite Fabricated by Solution Blow Spinning

*Liesel E. Cerna Nahuis, Cristhiane Alvim Valente, Danilo de Freitas Oliveira, Nara R. de Souza Basso, and José Antonio Malmonge**

**In this study, microfibers of poly(L-lactic-co-glycolic acid) (PLGA) and PLGA/polypyrrole (PPy) composite (90/10 wt%) are produced by using the solution blow spinning (SBS) technique. PPy is synthesized by the oxidative polymerization method using *p*-toluenesulfonic acid (*p*-TSA) as the dopant and $FeCl_3$ as the oxidant. The prepared PPy showed microfibers with globular particles morphology. Mixtures of porous and nonporous microfibers and microfibers incorporated with PPy are obtained. A wettability test shows that the PLGA and PLGA/PPy fibrous mats are hydrophobic. The electrical conductivity of the PLGA/PPy composite is of the same order as that of pure PLGA ($\approx 10^{-10}$ S cm$^{-1}$), indicating that the electrical percolation threshold is not reached for PPy loading of 10 wt%. The incorporation of PPy into PLGA microfibers improved the thermal stability of the composite and also increases the PLGA crystalline phase.**

## 1. Introduction

Conductive and biodegradable polymers have attracted considerable research attention worldwide because of their various industrial applications.[1,2] One such polymer is polypyrrole (PPy); PPy and its composites have attracted interest owing to their intrinsic conductivity, low toxicity, and good biocompatibility. Therefore, they enable biomedical applications involving the electrical stimulation of cells and tissues.[3,4] Furthermore, PPy is considered very promising for applications such as the regeneration of nerves and spinal cord tissues.

Several polymers, copolymers, and biodegradable polymer blends are used to produce and design polymeric biodegradable products for biomedical applications with varied life cycles and structures.[5,6] Poly(L-lactic-co-glycolic acid) (PLGA) is one such synthetic biodegradable polymer that has been approved by the Food and Drug Administration (FDA) for used in therapeutic devices. PLGA is used commonly owing to its easy of manufacture, adjustable degradation rate, and low inflammatory response.[7]

Fiber polymeric mats are used in biomedical applications such as wound dressing, tissue engineering, and enzyme immobilization.[8,5] Their porous structure results in a high surface-to-volume ratio that makes them suitable for medical applications.[9] Various processing techniques have been developed to fabricate micro- and nanofiber mats.[10] Electrospinning has been very well established for this purpose. Recently, Medeiros et al.[11] introduced solution blow spinning (SBS) as a simple alternative to electrospinning. SBS affords advantages such as higher fiber production rate, low production cost, and easy implementation. Furthermore, it can be used with various polymeric solutions regardless of their dielectric constant.[12] In SBS, a polymer solution is dragged toward a collector by a gas flow, and the solvent is evaporated during this process, and creates a nonwoven webs of polymer micro-and nanofibers, similar to those of the electrospinning technique. The fiber morphology, such as thickness and surface roughness, depends on variables such as carrier gas pressure, solution viscosity, and polymer type.[12]

In this work, SBS was used to produce microfibers mats of PLGA and PLGA/PPy composite. The mats were then examined using scanning electron microscopy (SEM), water contact angle, differential scanning calorimetry (DSC), thermogravimetric analysis (TG), X-ray diffraction (XRD), and electrical conductivity measurements by the two- and four-probe methods. Surprisingly, the PLGA and PLGA/PPy mats showed a mixture of porous and nonporous microfibers. The existence of pores favors cell growth and proliferation guide by PPy fibers and thus facilitates the formation of new biological tissues in tissue engineering.

## 2. Experimental Section

### 2.1. Materials

PLGA (Purasorb PLG8523 (85/15) L-lactide/glycolide copolymer; inherent viscosity = 2.38 dL g$^{-1}$ in chloroform) was supplied by Corbion Purac (Gorinchem, The Netherlands). Pyrrole (Py, purity: 98%), *p*-toluenesulfonic acid monohydrate (*p*-TSA), and

L. E. Cerna Nahuis, D. de Freitas Oliveira, J. Antonio Malmonge
Universidade Estadual Paulista (UNESP)
Faculdade de Engenharia
Campus de Ilha Solteira
Ilha Solteira, SP, Brazil
E-mail: mal@dfq.feis.unesp.br

C. Alvim Valente
Programa de Pós-graduação em Engenharia e Tecnologia de Materiais (PGETEMA)
Pontifícia Universidade Católica do Rio Grande do Sul
Porto Alegre, RS, Brazil

N. R. de Souza Basso
Escola de Ciências
Pontifícia Universidade Católica do Rio Grande do Sul
Porto Alegre, RS, Brazil

DOI: 10.1002/masy.201800030

 

ferric chloride ($FeCl_3$) were purchased from Sigma-Aldrich. Chloroform was purchased from Synth (Diadema, SP, Brazil).

### 2.2. Polypyrrole Synthesis

Py was purified by distillation before polymerization. All other chemicals were used without further purification. PPy was synthesized by the oxidative polymerization method using p-TSA as a dopant and $FeCl_3$ as an oxidant. In a typical polymerization reaction, Py (7.2 mmol) and *p*-TSA (32 mmol) were added to 20 mL of deionized water and stirred for 1 h at 0 °C. Then, 5 mL of $FeCl_3$ (12.3 mmol) aqueous solution was added dropwise to the solution. The reaction occurred under constant stirring for 24 h. PPy was filtered and washed several times with distilled water and ethanol. The final product was dried for 8 h at 80 °C.

### 2.3. SBS Solution Preparation

A PLGA solution (6% w/v) for SBS was prepared by dissolving PLGA granules in chloroform under magnetic stirring for 1 h at room temperature followed by an ultrasonic bath for 1 h. PLGA/PPy dispersions were prepared by the following procedure. First, PPy particles were dispersed in chloroform to 3% concentration (w/v) in an ultrasonic bath for 40 min. Then, the PPy dispersion was added to the PLGA solution under constant stirring for 20 min followed by an ultrasonic bath for 40 min. To produce a microfiber mat using these materials, 3 mL of the solution were placed in a disposable syringe (connected to a 20G spinal needle) coupled to an injection system. The injection rate and gas pressure used for the PLGA solution and PLGA-PPy suspension were 95 μL $min^{-1}$ and 207 kPa and 159 μL $min^{-1}$ and 152 kPa, respectively. Filtered air was used as the gas. The microfibers were collected in a cylinder (wrapped with aluminum foil) at 23 and 17 cm from the needle tip for PLGA and PLGA-PPy, respectively.

### 2.4. Characterization

The morphology of the obtained fibers was analyzed using an EVO LS15–Zeiss SEM. Before the analysis, the samples were attached to aluminum stubs with conductive carbon tape and sputtered with gold. Static water contact angle (WCA) measurements were performed using a goniometer (Phoenix 300, SEO). All images were captured 10 s (time zero) after the water droplets touched the sample surface to obtain measurements of unchanged sessile water droplets. Six drops of deionized water were applied to each membrane, and the mean and standard deviation of the WCA measurements were calculated. Thermogravimetric analysis (TA Instruments Model Q500) was conducted in the temperature range of 25–600 °C at a heating rate of 10 °C $min^{-1}$ in nitrogen atmosphere with a flow rate of 60 mL $min^{-1}$. Approximately 10 mg was used for each sample. DSC analyses (TA Instruments Model MDSC 292) were performed with a scan rate of 10 °C $min^{-1}$ in the temperature range of −10 to 200 °C under nitrogen atmosphere. XRD (Shimadzu XDR-6000) patterns were obtained using Cu-Kα radiation (wavelength: 1.5418 Å). Scans were conducted from $2\theta = 5°$ to 50° at a scan rate of 1° $min^{-1}$. PPy pellets were prepared by compacting PPy powder, and the electrical conductivity of the pellets was determined using the four-point probe method (Keithley Instruments Model 236 voltage source and HP34401 multimeter). PLGA and PLGA/PPy mats were compacted into pellets, and silver was painted on the pellet faces for forming better electrical contacts; then, the electrical conductivity of the pellets was determined using the two-point probe method (Keithley Instruments Model 247 voltage source and Model 610 electrometer).

## 3. Results and Discussion

SEM was used to evaluate the morphology of the synthesized PPy samples and the PLGA and PLGA/PPy mats produced by SBS. **Figure 1**a and b show SEM micrographs of PPy powder. Microfibers with globular particles were observed. The PPy morphology was strongly influenced by the experimental conditions.[13–19] Xia et al.[13] used an oxidative polymerization method and reported that the PPy morphology changed from particle to nanofiber upon changing the β-naphthalene sulfuric acid concentration and polymerization temperature. Ammonium persulfate was used as oxidant. Zhang et al.[14] reported that polypyrrole prepared by chemical oxidative polymerization of pyrrole in the presence of ionic, anionic and no-ionic surfactant, using ferric chloride as an oxidant, showed uniform sphere-like morphology with diameters in a narrow range between 35 and 60 nm. Wire- and ribbon-like nanostructures were found when ammonium persulfate was used as oxidizing agent. Wang et al.[15] have synthesized PPY nanoparticles with diameter 20–30 nm using ferric chloride as an oxidant and p-toluenesulfonate acid as a dopant. Although the current study uses a method similar to that used by Wang et al., the morphology obtained here is different because of the different sintheses conditons.

**Figure 2** shows micrographs of PLGA and PLGA/PPy mats. Mixtures of porous and nonporous fibers with different diameters are seen. Thicker microfibers contained nanopores. Bognitzki et al.[20] obtained similar results by electrospinning poly-L-lactide (PLLA) with dichloromethane as a solvent. Katsogiannis et al.[21] obtained polycaprolactone (PCL) porous microfibers by using a 90% (v/v) chloroform/dimethyl sulfoxide mixture. They found that the pore formation and pore morphology, including fiber diameter and surface morphology, depended on the electrospinning parameters, with applied voltage being the most important parameter. Rezabeigi et al.[22] produced porous polylactic acid (PLA) microfibers with various morphologies via the one-step electrospinning of liquid–liquid phase-separated PLA-dichloromethane-hexane systems. The differences in solvent evaporation rates caused composition changes in the electrospinning jet after ejection, leading to the formation of a two-phase region and, consequently, the formation of pores. Medeiros et al.[23] found that the type of solvent and polymer as well as moisture greatly influence the fiber morphology and pore formation when using electrospinning. In our case, we believe that when the polymer solution leaves the tip immediately the solvent is evaporated owing to its

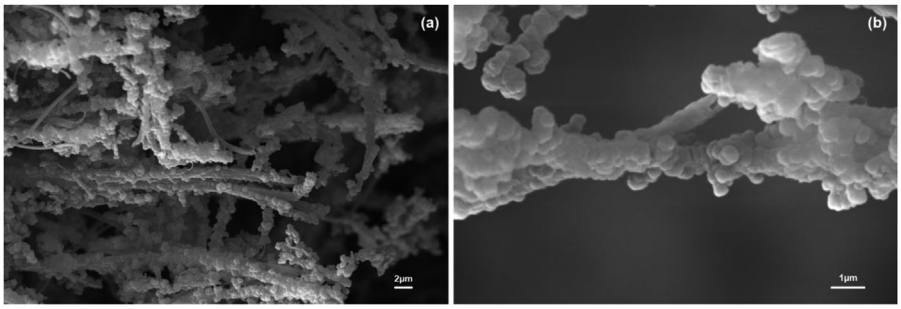


**Figure 1.** a) SEM image of PPy and b) higher magnification view of the same sample

high volatility (boiling point of chloroform is 61 °C). However, the solvent is not evaporated for thicker fibers as fast as it is for thin ones because the greater amount of the polymer in the jet. Consequently, a liquid phase can be created and pores can be formed after its evaporation. For PLGA/PPy mats, porous and nonporous microfibers of different diameters as well as fibers incorporated with PPy microfibers were observed. These results indicate that the PPy phase morphology is similar to that shown in Figure 1.

Surface hydrophobicity is a key factor governing cell response in biomedical applications, and it is evaluated by measuring the WCA of droplets on the surface.[24] The fibers mats obtained by SBS show low hydrophilicity (**Figure 3**a) with WCAs of 109° ± 2° (pure PLGA) and 104° ± 3° (PLGA/PPy (90:10)) (Figure 3b). The WCA reduces slightly with the addition of PPy particles. Electrospun polymer fibrous mats have been reported to show larger WCAs than dense polymer films.[25,26] This phenomenon is attributed to the surface morphology,[26,27] roughness, fiber porosity, fiber diameter, etc. that may result in different volumes of air being trapped at the fiber–water interface. The high WCA value for the PLGA fibrous mat in this study agrees with those reported in literature.[25,28]

The electrical conductivity of PPy and PLGA was of the order of 10–3 and 10–10 S cm$^{-1}$, respectively. PLGA/PPy showed electrical conductivity of the same order as pure PLGA. This insulating behavior indicates that the electrical percolation threshold is not reached for PPy loading of 10 wt %. It should be noted that the electrical conductivity measured herein is for volume resistivity and not for single fibers. The electrical conductivity measured for PLGA/PPy composites is comparable to those reported for different electrospun composites mats.[29,30]

**Figure 4** shows DSC thermograms of PPy, PLGA, and PLGA/PPy. The glass transition temperature (Tg) of PPy is strongly influenced by the experimental conditions. Jeeju et al.[31] reported that the Tg of PPy-Cl was ≈100 °C. Yeh et al.[32] found that the Tg of PPy-DBSA was 103 °C. Jeong et al.[33] reported that the Tg of PPy-ClO4 film is ≈268 °C. In the pure PPy synthesized in the present study, no Tg was observed in the temperature ranges studied. Furthermore, no significant

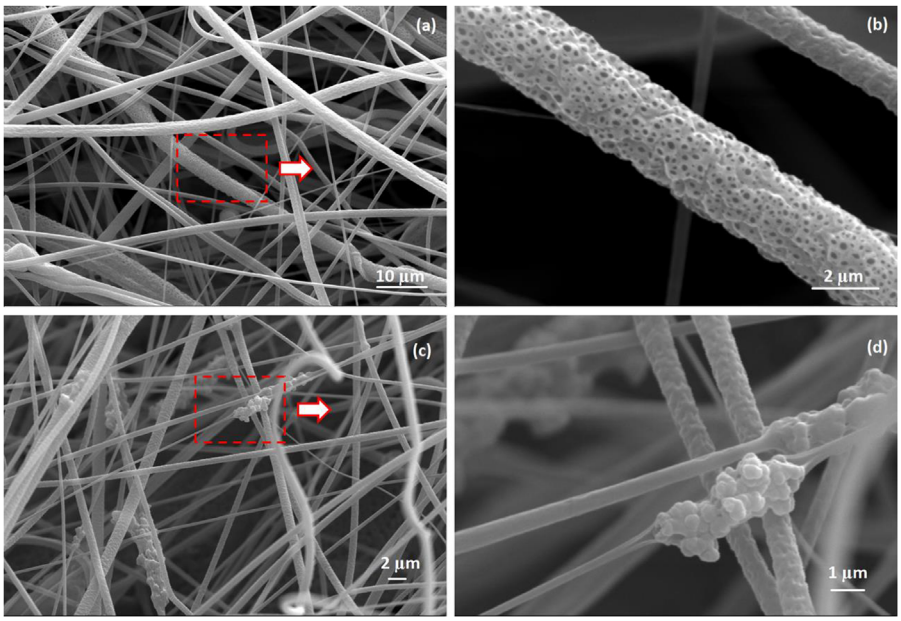


**Figure 2.** SEM micrographs of (a) PLGA and (c) PLGA/PPy fibers (b) and (d) Magnified views of the insets in (a) and (c), respectively.

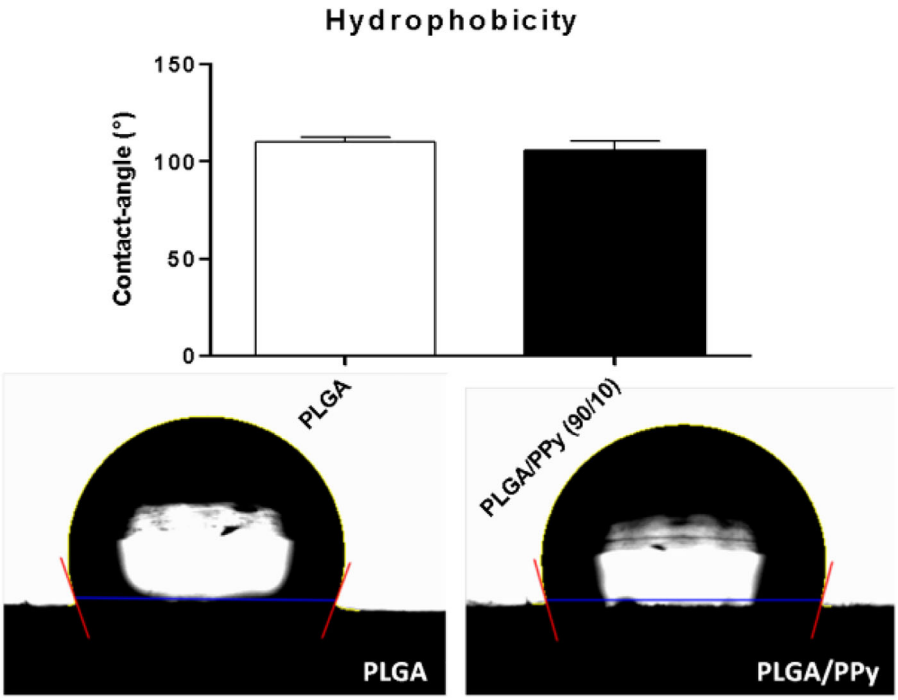


**Figure 3.** Contact angle for PLGA and PLGA/PPy (90/10 wt%).

change was seen in the Tg of PLGA (60 °C), and the melt temperature (158 °C), with 10 wt% of PPy in the composite. However, the enthalpy of fusion increased from 7.52 J $g^{-1}$ for pure PLGA to 10.76 J $g^{-1}$ for the PLGA/PPy composite. This result indicates that PPy particles contribute to an increase in the PLGA crystalline phase.

**Figure 5** shows XRD patterns of PPy, PLGA, and PLGA/PPy. The PLGA and PPy diffractograms show a broad diffraction band with a maximum centered at around $2\theta = 22°$ and $2\theta = 25°$, respectively. PLGA/PPy showed a narrower band than pure PLGA and PPy with a maximum centered at $2\theta = 16.6°$, indicating an increase in the PLGA crystalline phase; this agrees with the DSC measurements.

**Figure 6**a shows thermogravimetry (TG) profiles of PPy, PLGA, and PLGA/PPy, and Figure 6b shows their first derivative, that is, differential thermogravimetry (DTG). The TG curve of PPy showed three ranges of mass loss. The first one below 130 °C is attributed to water loss and other volatiles.[17] The second one in the range of 130–265 °C is attributed to the elimination of dopant anions from the PPy chains.[34] The third one above

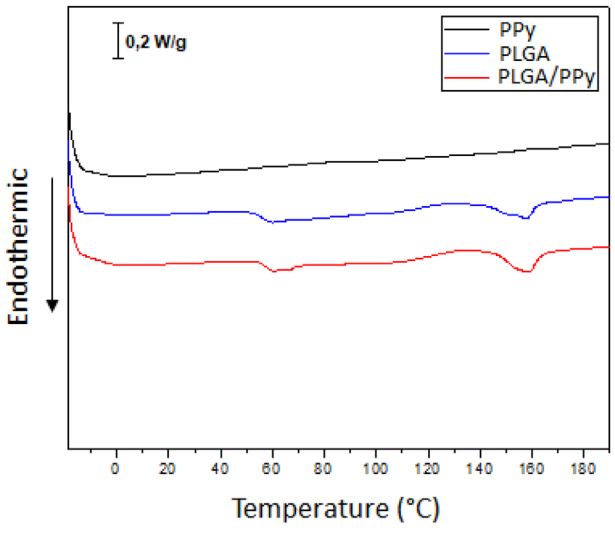


**Figure 4.** DSC curves of PPy, PLGA, and PLGA/PPy composite.

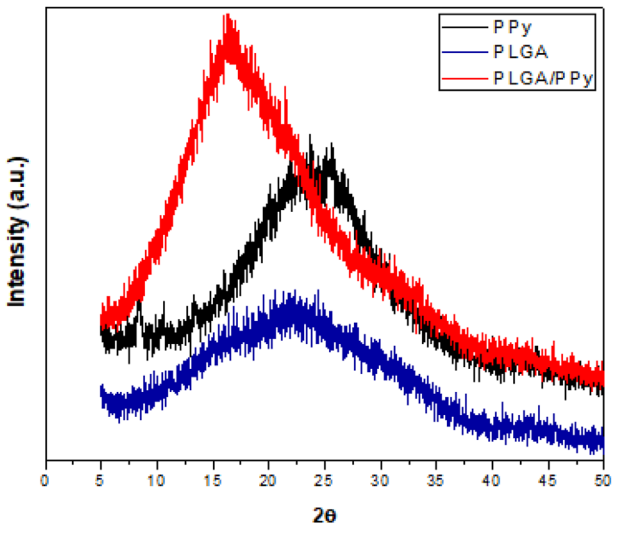


**Figure 5.** XRD patterns of PPy, PLGA, and PLGA/PPy samples.

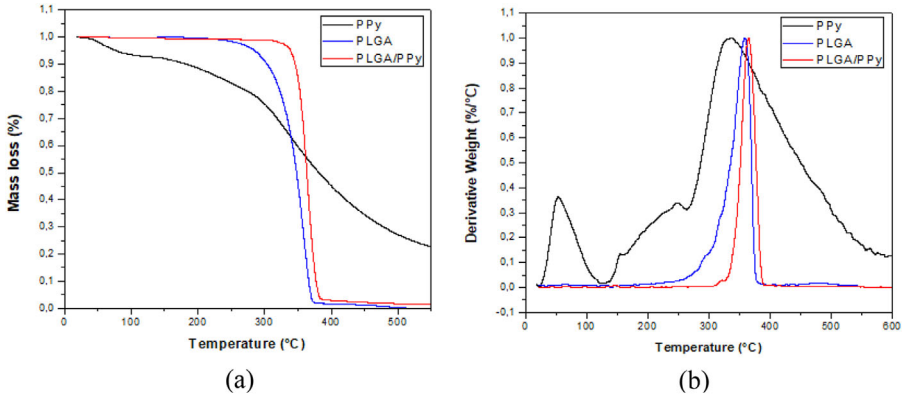


**Figure 6.** a) TG and (b) DTG curves of PPy, PLGA, and PLGA/PPy samples.

265 °C with maximum decomposition temperature rate (Tmd) at 335 °C is attributed to thermal decomposition of degradation or decomposition of the main PPy. PLGA shows only one weight loss stage between 200 and 390 °C with Tmd around 358 °C. This behavior agrees with that reported previously.[35]

The PLGA/PPy composite also showed a single step in the TG profile with Tmd around 364 °C. Its Tonset (i.e., initial decomposition temperature) is around 330 °C; this is ≈70 °C higher than that of pure PLGA. The addition of PPy particles improved the thermal stability of PLGA. Studies have reported that several types of inorganics nanoparticles improve the thermal stability of polymeric matrices via the large interfacial action between the polymer and the nanoparticles.[36] The thermal stability improvement found in this study can be also attributed to the increase in orderliness of PLGA chains supported by analysis of DSC and XRD measurements.

## 4. Conclusions

PPy synthesized by oxidative polymerization show an interesting morphology; microfibers with globular nanoparticles. Microfiber webs of PLGA and PLGA/PPy composite were obtained by SBS. The PLGA web shows a mixture of porous and nonporous microfibers of different diameters. The PLGA/PPy web showed the same morphology as well as fibers incorporated with PPy microfibers. The wettability test showed that the PLGA and PLGA/PPy webs are hydrophobic (WCAs of $109° \pm 2°$ for pure PLGA and $104° \pm 3°$ for PLGA/PPy composite). The electrical conductivity of the PLGA/PPy composite is similar to that of pure PLGA ($\approx 10^{-10}$ S cm$^{-1}$), and electrical percolation did not occur for 10% PPy content. The PLGA/PPy composite showed higher thermal stability than pure PLGA. The Tg of PLGA did not change with PPy content. However, the enthalpy of fusion increased significantly, indicating an increase in the PLGA crystalline phase.

## Acknowledgement

The authors would like to thank Coordenação de Aperfeiçoamento de Pessoal de Nível Superior (CAPES) and Conselho Nacional de Desenvolvimento Científico e Tecnológico (CNPq) for the financial support and scholarship.

## Keywords

biomaterials, polypyrrole, poly(L-lactic-co-glycolic acid), polymeric microfibers, solution blow spinning

[1] C. Yang, X. Wang, Y. Wang, P. Liu, *Powder Technol.* **2012**, *217*, 134.
[2] H. N. M. E. Mahmud, A. K. O. Huq, R. b. Yahyaa, *RSC Adv.* **2016**, *6*, 14778.
[3] K. S. U. Schirmer, D. Esrafilzadeh, B. C. Thompson, A. F. Quigley, R. M. I. Kapsa, G. G. Wallace, *J. Mater. Chem. B.* **2016**, *4*, 1142.
[4] L. Alvarez-Mejia, J. Morales, G. J. Cruz, M. G. Olayo, R. Olayo, A. Diaz-Ruiz, C. Rios, S. Sánchez-Torres, A. Morales-Guadarrama, O. Fabela-Sánchez, R. Mondragón-Lozano, H. Salgado-Ceballos, *J. Mater. Sci.: Mater. Med.* **2015**, *26*, 5541.
[5] A. S. Gerzson, D. C. Machado, R. R da Silva, C. A. Valente, R. M. Pagnoncelli, *J. Polym. Environ.* **2017**.
[6] B. D. Ulery, L. S. Nair, C. T. Laurencin, *J. Polym. Sci., Part B: Polym. Phys.* **2011**, *49*, 832.
[7] D. Arslantunali, T. Dursun, D. Yucel, N. Hasirci, V. Hasirci, *Med. Devices: Evidence Res.* **2014**, *7*, 405.
[8] A. M. Behrens, B. J. Casey, M. J. Sikorski, K. L. Wu, W. Tutak, A. D. Sandler, P. Kofinas, *ACS Macro Lett.* **2014**, *3*, 249.
[9] J. Zhou, Y. Wang, L. Cheng, Z. Wu, X. Sun, J. Peng, *Neural. Regen. Res.* **2016**, *11*, 1644.
[10] X. Wang, B. Ding, B. Li, *Mater. Today (Oxford, U. K.)* **2013**, *16*, 229.
[11] E. S. Medeiros, G. M. Glenn, A. P. Klamczynski, W. J. Orts, L. H. C. Mattoso, *J. Appl. Polym. Sci.* **2009**, *113*, 2322.
[12] J. E. Oliveira, E. A. Moraes, R. G. F. Costa, A. S. Afonso, L. H. C. Mattoso, W. J. Orts, E. S. Medeiros, *J. Appl. Polym. Sci.* **2011**, *122*, 3396.
[13] X. Xia, J. Yin, P. Qiang, X. Zhao, *Polymer* **2011**, *52*, 786.
[14] X. Zhang, J. Zhang, W. Song, Z. Liu, *J. Phys. Chem. B.* **2006**, *110*, 1158.
[15] J. Wang, S. Shen, J. Yin, *Synth. Met.* **2014**, *195*, 132.
[16] J. Pecher, S. Mecking, *Chem. Rev.* **2010**, *110*, 6260.
[17] A.T. Ramaprasad, D. Latha, V. Rao, *J. Phys. Chem. Solids* **2017**, *104*, 169.
[18] I. Sapurina, Y. Li, E. Alekseeva, P. Bober, M. Trchova, Z. Moravkov, J. Stejskal, *Polymer* **2017**, *113*, 247.
[19] S. Xing, G. Zhao, *J. Appl. Polym. Sci.* **2007**, *104*.
[20] M. Bognitzki, W. Czado, T. Frese, A. Schaper, M. Hellwin, M. Stinhart, A. Greiner, J. H. Wendorff, *Adv. Mater.* **2001**, *13*, 70.
[21] K. A. G. Katsogiannis, G. T. Vladisavljevic, S. Georgiadou, *J. Polym. Sci., Part B: Polym. Phys.* **2016**, *54*, 1878.

 

[22] E. Rezabeigi, M. Sta, M. Swain, J. McDonald, N. R. Demarquette, R. A. L. Drew, P. M. Wood-Adams, *J. Appl. Polym. Sci* **2017**, *134*, 44862.
[23] E. S. Medeiros, L. M. C. Mattoso, R. D. Offeman, D. F. Wood, W. J. Ortz, *Can. J. Chem*. **2008**, *86*, 590.
[24] J. Yang, Y. Wan, C. Tu, Q Cai, J. Bei, S. Wang, *Polym. Int*. **2003**, *52*, 1892.
[25] C. Wang, M. Wang, *J. Mater. Sci.: Mater. Med*. **2012**, *23*, 2381.
[26] Z. Ma, M. Kotakia, T. Yonga, W. Heb, S. Ramakrishna, *Biomaterials* **2005**, *26*, 2527.
[27] W. Cui, X. Li, S. Zhou, J. Weng, *Polym. Degrad. Stab*. **2008**, *93*, 731.
[28] Z. Ershuai, Z. Chuanshun, Y. Jun, S. Hong, Z. Xiaomin, Li. Suhua, W. Yongland, S. Lu, Y. Fanglian, *Mater. Sci. Eng. C* **2016**, *58*, 278.
[29] M. Wei, J. Lee, B. Kang, *J. Mead. Macromol. Rapid Commun*. **2005**, *26*, 1127.
[30] C. Merlini, A. Pegoretti, T. M. Araujo, S. D. A. S. Ramoa, W. H. Schreiner, G. M. O. Barra, *Synth. Met* **2016**, *213*, 34.
[31] P. P. Jeeju, S. J. Varma, P. A. F Xavier, A. M. Sajimol, S. Jayalekshmi, *Mater. Chem. Phys* **2012**, *134*, 803.
[32] J. M. Yeh, C. P. Chin, S. Chang, *J. Appl. Polym. Sci*. **2003**, *88*, 3264.
[33] R. A. Jeong, G. J. Lee, H. S. Kim, K. Ahn, K. Lee, K. H. Kim, *Synth. Met*. **1998**, *98*, 9.
[34] J. Hazarika, A. Kumar, *J. Phys. Chem. B* **2017**, *121*, 6926.
[35] H. Fouad, T. Elsarnagawy, F. N. Almajhdi, K. A. Khalil, *Int. J. Electrochem. Sci*. **2013**, *8*, 2293.
[36] K. Chrissafis, D. Bikiaris, *Thermochim. Acta* **2011**, *523*, 01.